

Semi-automatic detection of Gd-DTPA-saline filled capsules for colonic transit time assessment in MRI

Christian Harrer^a, Sonja Kirchhoff (MD)^b, Andreas Keil^{a,c}, Chlodwig Kirchhoff (MD)^c,
Thomas Mussack (MD)^c, Andreas Lienemann (MD)^b, Maximilian Reiser (MD)^b, Nassir Navab^a

^aComputer Aided Medical Procedures (CAMP), Technische Universität München, Germany¹

^bInstitute of Clinical Radiology, University Hospital Munich – Großhadern, Germany

^cDepartment of Surgery, University Hospital Munich – Innenstadt, Germany

ABSTRACT

Functional gastrointestinal disorders result in a significant number of consultations in primary care facilities. Chronic constipation and diarrhea are regarded as two of the most common diseases affecting between 2% and 27% of the population in western countries¹⁻³. Defecatory disorders are most commonly due to dysfunction of the pelvic floor or the anal sphincter. Although an exact differentiation of these pathologies is essential for adequate therapy, diagnosis is still only based on a clinical evaluation¹. Regarding quantification of constipation only the ingestion of radio-opaque markers or radioactive isotopes and the consecutive assessment of colonic transit time using X-ray or scintigraphy, respectively, has been feasible in clinical settings⁴⁻⁸. However, these approaches have several drawbacks such as involving rather inconvenient, time consuming examinations and exposing the patient to ionizing radiation. Therefore, conventional assessment of colonic transit time has not been widely used. Most recently a new technique for the assessment of colonic transit time using MRI and MR-contrast media filled capsules has been introduced⁹. However, due to numerous examination dates per patient and corresponding datasets with many images, the evaluation of the image data is relatively time-consuming. The aim of our study was to develop a computer tool to facilitate the detection of the capsules in MRI datasets and thus to shorten the evaluation time. We present a semi-automatic tool which provides an intensity, size¹⁰, and shape-based^{11,12} detection of ingested Gd-DTPA-saline filled capsules. After an automatic pre-classification, radiologists may easily correct the results using the application-specific user interface, therefore decreasing the evaluation time significantly.

Keywords: MRI, colon transit time, segmentation, classification, shape, functional imaging, PCA

1. INTRODUCTION

The number of patients suffering from functional gastrointestinal disorder like chronic constipation has significantly increased¹⁻³ over the past few years. Different forms of chronic constipation have to be differentiated: a) normal-transit constipation and b) slow-transit constipation with pathological, prolonged transit times. Those disorders are most usually due to dysfunction of the pelvic floor or the anal sphincter. The differentiation of these pathologies is essential for adequate therapy. But conventional assessment of colonic transit time has not been widely used due to repeated exposure to ionizing radiation. Recently, a new technique for the assessment of colonic transit time using MRI and Gd-DTPA-saline-filled capsules (see Figure 1) was introduced in the literature⁹. Due to numerous examinations and images/examination, data-evaluation is time-consuming. Therefore, the aim was to develop a computer-aided detection tool prototype to facilitate the finding of the capsules in MR-datasets, thus to shorten the evaluation time of the colonic transit.

¹ Website: <http://campar.cs.tum.edu>

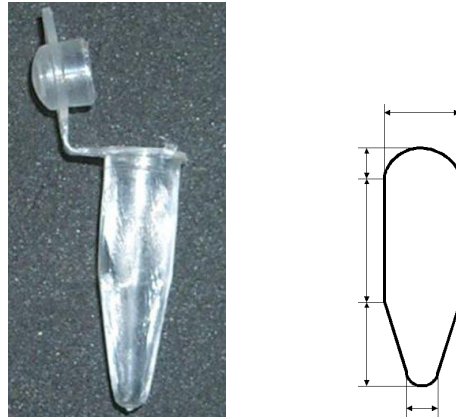


Fig. 1: Enlarged image and model of the capsule being ingested after filled with contrast agent and saline.

2. METHODS

Image data was available in T1- and T2-weighted sequences. However, T2-weighted images turned out to be too coarse and differentiation between the capsules and certain tissue was too low to perform a reliable segmentation (see Figure 2). Voxel intensity would have been a rather weak classification criterion if applied to T2-weighted images, thus our focus was set on the capsule detection in T1-weighted MR images.

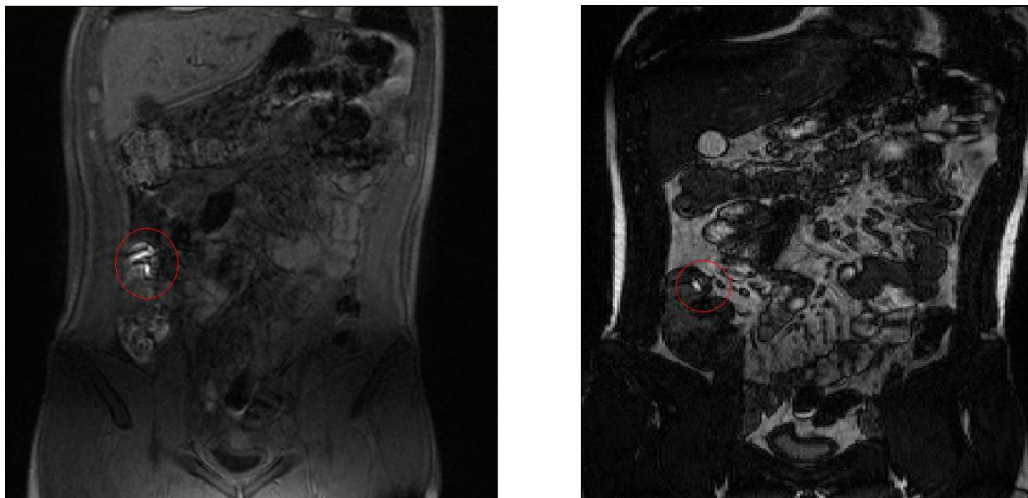


Fig. 2: T1-weighted (left) and T2-weighted (right) images in coronal orientation with red marked capsules.

An interactive slice browser (see Figure 3) was developed providing a quick overview of the image data. The user selects a region of interest, where an automated screening for the capsules is performed. After screening, the detected objects are shown colored in the corresponding slices. False negative and false positive findings can be added or removed, respectively, by the radiologist. Several image processing methods like signal intensity thresholding, connected component analysis, and principal component analysis were applied enabling the combination of several criteria for an automatic capsule detection. Signal intensity, size, and shape were taken into account in order to achieve acceptable detection results.

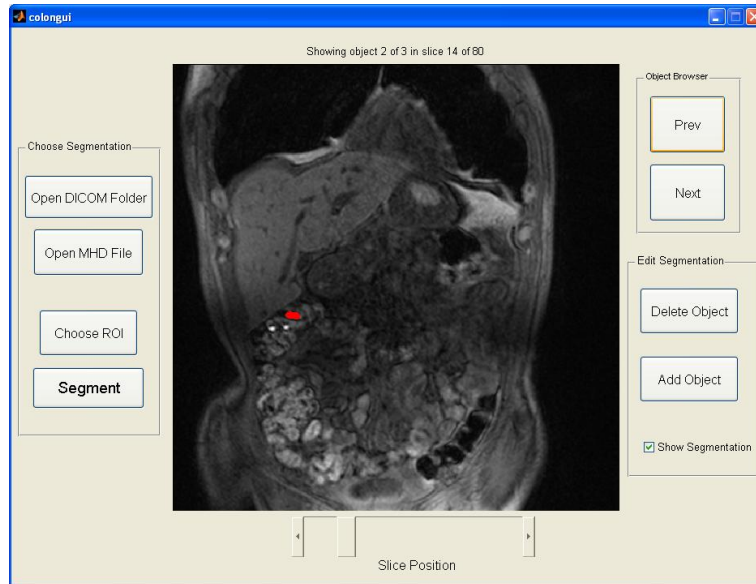


Fig. 3: User interface with automatic classification and correction possibilities.

2.1 Thresholding

For better visibility in MR-image volumes, the capsules ingested by the patients were filled with Gd-DTPA-saline-mixture yielding a fairly high signal intensity. Thus, intensity thresholding¹⁰ was applied as a first segmentation step. A suitable threshold value was selected by manually looking for capsule-images in a certain number of volumes.

However, selecting a threshold value for segmenting the contrast agent filled capsules is rather difficult because the cross section of the capsule and thus the visible signal of contrast agent may vary. Since other classification criteria will be applied in the following stages of the capsule detection, the threshold value is chosen so that usually all capsules are segmented, leading to many false positives but no false negative findings at this stage (see Figure 4).

Although intensity thresholding on its own provides only a very weak criterion for segmenting capsules, it is a very useful and computationally inexpensive first step because it preprocesses the data so that more elaborate classification criteria based on shape- and volume-analysis can then be applied.

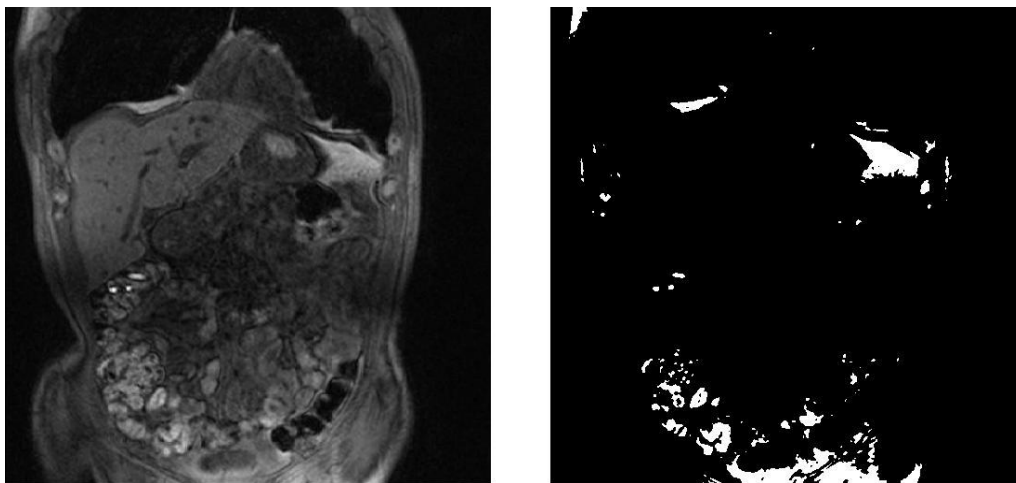


Fig. 4: Original and thresholded T1-weighted MR-image. Three capsules are located in the middle-left area of the slice. They are properly segmented but a lot of high-intensity artifacts (= false positives) are remaining when using the current threshold value).

2.2 Connected component analysis for volume measurements

After having segmented voxels with high intensity, a connected components analysis¹⁰ has to be performed in order to extract separate objects. This algorithm systematically scans the thresholded data volume, assigning labels to segmented voxels. Voxels in the neighborhood of already scanned image points are provided with the same label yielding a partition of the segmented volume into a certain number of scatter plot, whereas the points of each disjoint cloud bear the same label (see Figure 5). The resulting objects can then be analyzed with respect to their volume as well as their shape.

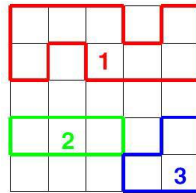


Fig.5: Schematic view of the connected components analysis.

The exact dimensions of the real capsules are known and are used to compute their volume (approx. 520mm^3). An extracted object's volume can then be used as a criterion of discrimination. Since the resolution of the MR volumes is given, the approximate real volume of an object occupying one voxel in the image can be computed. This is done by primarily counting the number of an object's voxels and multiplying it with the volume-per-voxel-ratio deriving from above, resulting in the possibility of calculating the actual volume of the segmented objects. However, due to anisotropic image resolution, the voxel count of one capsule may strongly vary and the range of acceptable object voxel counts has to be set rather wide (see Figure 6). In our study relevant image data was only available at a resolution of $0.78\text{mm} : 0.78\text{mm} : 2\text{mm}$ since the MR-images were acquired in terms of a feasibility study to assess colon transit with capsules in MR before the software tool for data analysis was considered and developed. This lead to a great dependence of the voxel count on the capsule's position with respect to the coordinate axes of the imaging system. Image data with homogeneous resolution would most likely lead to much better classification results because the number of voxels per capsule could be defined more precisely, yielding a more powerful classification criterion.

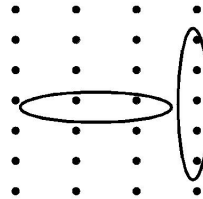


Fig. 6: Highly anisotropic resolution impedes exact volume and shape measures. In this case two objects of the same size occupy two and five voxels, respectively, in a slice with highly anisotropic resolution.

2.3 Principal component analysis for shape analysis

Since the intensity as well as the volume tests performed up to this stage can only use weak conditions due to the highly varying image representation of the capsules, a last, shape-based criterion is added to the analysis. Exact representation of the capsules as a computer model and using this as a template for comparison with each of the segmented objects would be too time-consuming in this application. Furthermore, the high variation in the image representation of the capsules mentioned above implies that comparing possible capsule candidates to an exact model would probably lead to a high number of false negative findings. Therefore a more general approach is chosen concentrating on the basic geometrical properties of the segmented objects. The capsules are modeled as ellipsoids with a ratio of the three main axes (= principal components) $a:b:c = 1:1:4$ deriving from the actual measurements of the capsules (see Figure 7).

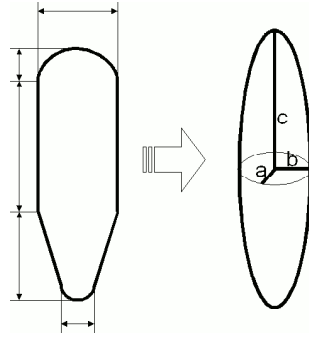


Fig. 7: Approximation of capsule shape by ellipsoid with three principal components.

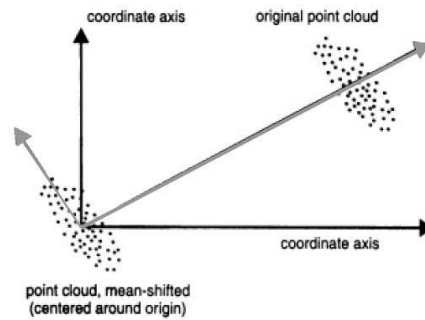


Fig. 8: 2D-example of an original and shifted (demeaned) point cloud with principle axes (grey) obtained by applying PCA. Shifting is necessary in order to make the results independent of the object's position in the coordinate system.

The principal axes of one segmented object are computed using principal components analysis (PCA) and then compared to the ratios mentioned above. The principal components analysis^{11,12}, in the literature also referred to as proper orthogonal decomposition (POD) or Karhunen-Loève transformation is a method used in many scientific fields such as for statistical data analysis and image processing. The idea behind this algorithm is to obtain a low dimensional description of the main structural information contained in a large number of data points. In our case, where the data represents a scatter plot in 3D-space, PCA tries to treat this point cloud as a representation of an ellipsoid which can be exactly described by the directions and lengths of its main axes, the principal components. The PCA algorithm works as follows:

Let X be the set of points of an segmented object assembled in a matrix

$$X = \begin{pmatrix} x_1 & x_2 & x_3 & \dots \\ y_1 & y_2 & y_3 & \dots \\ z_1 & z_2 & z_3 & \dots \end{pmatrix},$$

(x_1, y_1, z_1) being the coordinates of the first point of a segmented object etc. This point set is first demeaned using the mean x - y - and z -values $\bar{x}, \bar{y}, \bar{z}$ in order to obtain a point set \tilde{X} with its center of mass at the origin (see Figure 8):

$$\tilde{X} = \begin{pmatrix} x_1 - \bar{x} & x_2 - \bar{x} & x_3 - \bar{x} & \dots \\ y_1 - \bar{y} & y_2 - \bar{y} & y_3 - \bar{y} & \dots \\ z_1 - \bar{z} & z_2 - \bar{z} & z_3 - \bar{z} & \dots \end{pmatrix}$$

This point set's principal axes can then be obtained by computing the singular value decomposition (SVD) of its covariance matrix $C = \tilde{X}^T \cdot \tilde{X}$

$$C = \tilde{X}^T \cdot \tilde{X} = U \cdot D \cdot U^T,$$

where U is an orthogonal matrix whose columns contain the principal axes' directions and D being a diagonal matrix with those axes' lengths (sorted by their magnitude):

$$D = \begin{pmatrix} c & & \\ & b & \\ & & a \end{pmatrix}, \quad c \geq b \geq a$$

If the analyzed object is the image of a colon capsule, the ratio $a:b:c$ should be roughly 1:1:4, enabling us to introduce an additional shape based classification criterion for capsule detection. As error measure, we use

$$E = \left| \frac{a}{b} - 1 \right| + \left| \frac{c}{a} - 4 \right|,$$

penalizing deviations from the assumed ellipsoid's axes ratios which were obtained by first calculating the volume of the original capsules and then generating an ellipsoid with similar length and the same volume. Only objects with E not exceeding a certain threshold were accepted as possible capsules.

3. RESULTS

As mentioned before, all of the three criteria used (intensity, volume, and shape) are subject to high variance. However, the shape-based measure turned out to be quite accurate. This was the reason for pursuing a multi-stage approach of sorting out object candidates based on weak conditions for intensity and volume and then using the (computationally most expensive but also most accurate) shape criterion in the last step.

In an evaluation experiment on seven datasets more than 50% of the visible capsules were automatically detected by our algorithm, leaving only the false positive findings to the radiologist to be removed (Figure 9). The inhomogeneous resolution of the available image data turned out to be the greatest challenge for the segmentation task. Even though all calculations were done taking the different resolution in each coordinate direction into account, the resulting inhomogeneous distribution of the points inside each point cloud led to sometimes highly varying values for the corresponding volume and shape measures. Only the combination of several criteria yielded acceptable results. However, when choosing the threshold values, emphasis was set on minimizing the number of false negative findings. When the volume and shape ranges were set too narrow, an undesired side effect of too many objects represent the images of the real capsules are discarded. Since we designed our software tool with a function providing the opportunity to delete obvious false positives by simply clicking on them, a relatively high number of false positives is tolerable.

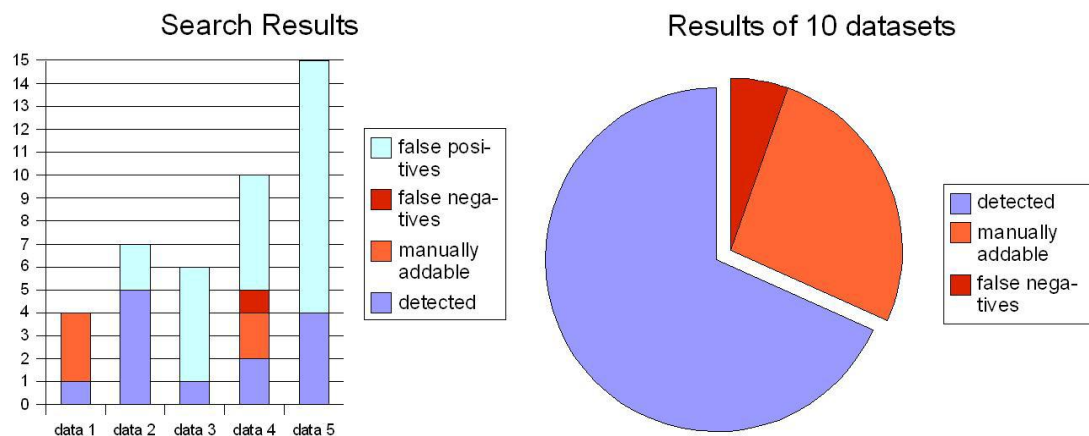


Fig. 9: Results of the study used to evaluate the detection results.

4. CONCLUSION

The implemented user interface presents a great improvement compared to a manual evaluation performed by the radiologist in terms of scrolling through all images of one dataset looking for the capsules. Capsule candidates are extracted automatically and false positive findings can be removed by the radiologist in very fast and effective way. The average time needed to correctly locate all capsules in one dataset was considerably decreased with a resulting approximate time effectiveness of 2-3 minutes per dataset. The faster and more comfortable evaluation provided by the computer-aided detection tool presented in this work enables a more detailed transit time assessment and offers the possibility of using this new MR-based method during clinical routine scanning.

Further work will include a redefinition of the MR protocol especially in order to acquire data with isotropic resolution. This will probably improve the possibilities of volume and shape evaluation, as described above, and also will enable the incorporation of further classification criteria possibly leading to further reduction of the number of false positive findings.

REFERENCES

- [1] Lembo, A. and Camilleri, M., "Chronic constipation," *N. Engl. J. Med.* 349, 1360-1368 (2003)
- [2] Almy, T. P.: "Digestive disease as a national problem. II. A white paper by the Gastroenterological association," *Gastroenterology* 53, 821-833 (1969)
- [3] Harvey, R. F., Salith, S. Y. and Read, A. E., "Organic and functional disorders in 2000 gastroenterology outpatients," *Lancet* I, 632-634 (1983)
- [4] Hinton, J., Lennard-Jones, J. and Young A., "A new method of studying gut transit times using radiopaque markers," *Gut* 10, 842-847 (1969)
- [5] Eastwood, H. D., "Bowel transit time studies in the elderly: Radiopaque markers in the investigation of constipation," *Gerontol. Clin.* 14, 154-159 (1972)
- [6] Martelli, H., Devroede, G., Arhan, P. and Duguay, E., "Mechanisms of idiopathic constipation: outlet obstruction," *Gastroenterology* 75, 623-632 (1978)
- [7] Waite, A., Devroede, G., Duranceau, A. et al., "Constipation with colonic inertia: A manifestation of systemic disease?" *Dig. Dis. Sci.* 28, 1025-1033 (1983)
- [8] Arhan, P., Devroede, G., Jehannu, B. et al., "Segmental transit time," *Dis. Colon Rectum* 24, 625-629 (1981)
- [9] Buhmann(=Kirchhoff), S., Kirchhoff, C., Ladurner, R., Mussack, T., Reiser, M. F. and Lienemann, A., "Assessment of colonic transit time using MRI: A feasibility study," *Eur. Radiol.* (Epub ahead of print), (2006)

- [10] Gonzalez, R. C. and Woods, R. E., [Digital Image Processing], Prentice Hall, chapters 9 and 10 (2002)
- [11] Chatterjee, A., "An introduction to the proper orthogonal decomposition," Current Science 78(7), 808-817 (2000)
- [12] Pearson, K., "On lines and planes of closest fit to systems of points in space," Philosophical Mag. (1901)